Genes & Diseases (2021) 8, 531–544

Available online at www.sciencedirect.com

ScienceDirect

journal homepage: http://ees.elsevier.com/gendis/default.asp

FULL LENGTH ARTICLE

Bone morphogenetic protein 4 (BMP4) promotes hepatic glycogen accumulation and reduces glucose level in hepatocytes through mTORC2 signaling pathway

Liqin An [a,1], Qiong Shi [a,1], Ying Zhu [a], Hao Wang [a], Qi Peng [a], Jinghong Wu [a], Yu Cheng [b], Wei Zhang [a], Yanyu Yi [a], Zihao Bao [a], Hui Zhang [a], Yetao Luo [c], Jiaming Fan [a,*]

[a] *Ministry of Education Key Laboratory of Diagnostic Medicine, Department of Clinical Biochemistry, School of Laboratory Medicine, Chongqing Medical University, Chongqing, 400016, PR China*
[b] *Department of Clinical Laboratory, The Second Affiliated Hospital of Chongqing Medical University, Chongqing, 400010, PR China*
[c] *Clinical Epidemiology and Biostatistics Department, Department of Pediatric Research Institute, Children's Hospital of Chongqing Medical University, Chongqing, 400014, PR China*

Received 24 August 2020; received in revised form 14 October 2020; accepted 5 November 2020
Available online 13 November 2020

KEYWORDS
BMP4;
Glucose metabolism;
Glycogen accumulation;
mTORC2 signaling;
Non-alcoholic fatty liver disease (NAFLD)

Abstract Liver is an important organ for regulating glucose and lipid metabolism. Recent studies have shown that bone morphogenetic proteins (BMPs) may play important roles in regulating glucose and lipid metabolism. In our previous studies, we demonstrated that BMP4 significantly inhibits hepatic steatosis and lowers serum triglycerides, playing a protective role against the progression of non-alcoholic fatty liver disease (NAFLD). However, the direct impact of BMP4 on hepatic glucose metabolism is poorly understood. Here, we investigated the regulatory roles of BMP4 in hepatic glucose metabolism. Through a comprehensive analysis of the 14 types of BMPs, we found that BMP4 was one of the most potent BMPs in promoting hepatic glycogen accumulation, reducing the level of glucose in hepatocytes and effecting the expression of genes related to glucose metabolism. Mechanistically, we demonstrated that BMP4 reduced the hepatic glucose levels through the activation of mTORC2 signaling pathway *in vitro* and *in vivo*. Collectively, our findings strongly suggest that BMP4 may play an essential role in regulating hepatic glucose metabolism. This knowledge should aid us to understand the molecular pathogenesis of NAFLD, and may lead to the development of novel therapeutics by

* Corresponding author. Ministry of Education Key Laboratory of Diagnostic Medicine, Department of Clinical Biochemistry, School of Laboratory Medicine, Chongqing Medical University, No. 1 Medical School Road, Yuzhong District, Chongqing, 400016, China.
E-mail address: fanjiaming1988@cqmu.edu.cn (J. Fan).
Peer review under responsibility of Chongqing Medical University.
[1] Contributed equally.

https://doi.org/10.1016/j.gendis.2020.11.004

exploiting the inhibitory effects of BMPs on hepatic glucose and lipid metabolism.

Introduction

Liver is an important organ to regulate glucose and lipid metabolism.[1,2] When mammalians uptake energy diet, liver preferentially uses glycolysis to generate energy, while excessive glucose is stored in the form of hepatic glycogen (glycogen synthesis) and/or converted into triglycerides. The prolonged excess in energy supplies, especially in the form of high carbohydrates or fat, rapidly induces the development of fatty liver.[3,4] When an imbalance between energy intake and energy expenditure occurs, ectopic fat accumulation occurs in tissues or organs not designed to accumulate fat. Nonalcoholic fatty liver (NAFLD) is an example of ectopic fat accumulation, which is usually concomitant with increased gluconeogenesis, decreased glycogen synthesis, and inhibition of insulin signaling.[4–6]

Bone morphogenetic proteins (BMPs), their antagonists, and BMP receptors (BMP-Rs) are involved in controlling a broad range of biological functions including cell proliferation, stem cell differentiation, cell fate decision, and apoptosis in many different types of cells and tissues during embryonic development and postnatal life.[7–10] As a member of TGF-β superfamily, BMPs are precursor proteins with N-terminal signal peptides and C-terminal mature peptides. In the canonical signaling pathway, BMPs bind to their cognate receptors on the cell membrane (BMP-Rs), lead to phosphorylate and activate BMPR-specific Smad1/5/8 in the cells, form a complex with Smad4, enter into the nucleus, bind to the promoter sequences of target genes, and regulate the transcription of the target gene.[8,11,12] In recent years, it has been shown that several BMPs, especially BMP4, play an important role in the energy metabolism. BMP4 significantly reduces the weight and volume of white fat in mice through PGC1α, and changes the white fat cells into brown fat cells, promotes M2 macrophage to induce the formation of beige fat and improves insulin sensitivity through p38/MAPK/STAT6/PI3K-AKT signaling pathway, and plays a protective effect against diet-induced obesity and diabetes.[13,14] BMP4 has been also shown to increase the whole bodies energy consumption, reduce liver fat, and reduce fat tissue inflammation.[15,16]

We previously found that BMP4 was highly expressed in the middle and late stage of NAFLD.[17] Exogenous BMP4 was shown to significantly reduce the accumulation of fat in the liver, serum levels of triglycerides and body weight of mice, and inhibit the development of NAFLD by down-regulating mTORC1 signal activity. However, little is known about whether and how BMP4 exerts any effect on hepatic glucose metabolism. In this study, we found that BMP4 was one of the most potent BMPs in promoting hepatic glycogen accumulation among 14 types of BMPs. Mechanistically, we demonstrated that BMP4 increased the hepatic glycogen and reduced the hepatic glucose levels through the activation of mTORC2 signaling pathway. Thus, our findings strongly suggest that BMP4 may play an important role in regulating hepatic glucose metabolism. Our study should help us to understand the molecular pathogenesis of NAFLD, and the effects of BMPs on hepatic glucose and lipid metabolism.

Materials and methods

Cell culture and chemicals

HEK-293 derivative 293pTP and RAPA cells were previously described.[18,19] Mouse primary hepatocytes (MPH) cells were obtained from 4-week old C57BL/6J mice using the type I collagenase/liver perfusion protocol as described.[9,20] All cells were maintained in complete Dulbecco's modified Eagle's medium (DMEM) supplemented with 10% fetal bovine serum (Lonsa Science SRL), 100 units of penicillin and 100 μg of streptomycin at 37 °C in 5% CO_2. Unless indicated otherwise, all chemicals were purchased from Sigma–Aldrich (St Louis, MO, USA), Thermo Fisher Scientific (Waltham, MA, USA), Solarbio (Beijing, China).

Total RNA isolation and touchdown-quantitative real-time PCR (TqPCR) analysis

Total RNA from both cells and freshly-prepared liver tissues was isolated by using the TRIZOL Reagent (Invitrogen, China) as described.[21–23] Briefly, the freshly prepared mouse liver tissues at the indicated development stages (n = 5, C57BL/6J male mice for each time point) or the NAFLD model was dissected out, minced, and ground in the TRIZOL Reagent. MPH cells were treated with different conditions for varied durations and lysed in TRIZOL Reagent for total RNA isolation. Total RNA was subjected to reverse transcription with hexamer and M-MuLV reverse transcriptase (New England Biolabs, Ipswich, MA). The cDNA products were further diluted and used as PCR templates. Gene-specific PCR primers were designed by using Primer3 program (Table 2). TqPCR was carried out by using 2x SYBR Green qPCR Master Mix (Bimake, Shanghai, China) on a CFX-Connect unit (Bio-Rad Laboratories, Hercules, CA) as described. All TqPCR reactions were done in triplicate. Gapdh was used as a reference gene. Quantification of gene expression was carried out by using the 2-ΔΔCq method as described.

Construction and amplification of recombinant adenoviruses

Recombinant adenoviruses were generated by using the AdEasy technology.[10,24–27] Briefly, the full-length coding

Table 1 Formula and fatty acid composition of control (10% fat) and high fat (45% fat) diets.

	MD10% Fat	MD45% Fat
Energy Composition	100	100
Protein	20	20
Carbohydrate	70	35
Fat	10	45
Composition of fatty acid	100	100
Saturated (%)	28.7	40.3
Monounsaturated (%)	32.7	40.4
Polyunsaturated (%)	38.6	19.3
Type of fat (gm)	45	202.5
Lard	20	177.5
Soybean Oil	25	25
Fatty acid profile (gm)	42.2	190.6
C2, Acetic	0	0
C4, Butyric	0	0
C6, Caproic	0	0
C8, Caprylic	0	0
C10,Capric	0.0	0.1
C12,Lauric	0.0	0.1
C14,Myristic	0.3	2.1
C15	0.0	0.2
C16,Palmitic	7.9	47.1
C16:1,Palmitoleic	0.4	3.4
C16:2	0	0
C16:3	0	0
C16:4	0	0
C17	0.1	0.6
C17:1	0	0
C18,Stearic	3.8	26.5
C18:1,Oleic	13.4	73.5
C18:2,Linoleic	14.6	32.4
C18:3,Linolenic	1.4	2.1
C18:4, Stearidonic	0	0
C20,Arachidic	0.0	0.2
C20:1	0.0	0.1
C20:2	0.1	0.4
C20:3	0.0	1.1
C20:4,Arachidonic	0.1	0.7
C20:5, Eicosapentaenoic	0	0
C21:5	0	0
C22, Behenic	0	0
C22:1, Erucic	0	0
C22:4, Clupanodonic	0	0
C22:5,Docosapentaenoic	0.0	0.2
C22:6, Docosahexaenoic	0	0
C24, Lignoceric	0	0
C24:1	0	0

regions of 14 human BMPs were PCR amplified for generating recombinant adenoviral plasmid pAd-Bs, the resultant shuttle vectors were used to generate recombinant adenoviral vectors through homologous recombination with the adenoviral backbone vector in bacterial BJ5183, which were subsequently used to generate recombinant adenoviruses, namely Ad-B2 through Ad-B15 in 293 or its derivative lines 293pTP or RAPA cells. The resulting 14 Ad-Bs adenoviruses that also co-express GFP as a marker for tracking infection efficiency.[10,26]

For the construction of the adenoviral vectors expressing siRNAs targeting mouse Bmp4, we employed our recently developed pSOS and related systems, in which siRNA expression is driven by the converging human U6 and H1 promoters.[22,28–31] Three siRNA sites targeting mouse *Bmp4* were designed by using Invitrogen's BLOCK-iTRNAi Designer and/or Dharmacon Horizon Discovery's siDESIGN programs (Table 3) and subcloned into a single adenoviral shuttle vector. The resulting recombinant adenoviral vector was used to generate adenovirus Ad-siB4, which expresses the three siRNAs, and also co-expresses the RFP marker gene. Adenoviral vector expresses RFP (Ad-RFP) or GFP(Ad-GFP) alone was used as a mock adenovirus control.[32,33] Fluorescence signals were documented under a fluorescence microscope after 48h. For all adenoviral infections, polybrene (8 μg/ml) was added to enhance infection efficiency.[34]

For the *in vivo* direct injection studies, high titer adenoviruses (Ad-B4 and Ad-GFP) were prepared by using CsCl gradient ultracentrifugation and dialyzed immediately before use as previously described.[17,25,35–38]

H & E staining and immunohistochemical (IHC) staining

The retrieved mouse liver was fixed in 4% paraformaldehyde overnight, and subjected to paraffin embedding and sectioning. The sections were deparaffinized, rehydrated and subjected to H & E staining and IHC staining as described.[18,23,39] Briefly, the sections were subjected to deparaffnization, followed by antigen retrieval and immunostaining with an AKT (1:200 dilution; Gene Tex; Cat# GTX121937), phospho-AKT Ser473 (1:200 dilution; Gene Tex; Cat# GTX128414), GSK-3β(1:100 dilution; Bioss; Cat# bs-0028R), phospho-GSK-3βSer9 (1:100 dilution; Bioss; Cat# bs-2066R), FOXO1 (1:100 dilution; Bioss; Cat# bs-2537R) and phospho-FOXO1 Ser319 (1:100 dilution; Bioss; Cat# bs-20095R). Control rabbit IgG (1:200; cat. no. 011-000-003; Jackson ImmunoResearch Laboratories, Inc.) was used as a negative control. Each assay condition was done in triplicate. Staining results were recorded under light microscope (magnification, x400).

Periodic acid-schiff (PAS) staining (glycogen storage)

PAS staining assay was carried out as described.[23,40-42] In order to eliminate the influence of diet-based glycogen, mice were fasted for 6-8 h before the experiment. The harvested tissues were fixed and paraffin embedded. Tissue sections were deparaffinized, rehydrated and then subjected to PAS staining. For the cultured cells, subconfluent MPH cells were seeded in 24-well culture plates with various treatments (e.g., infected with Ad-Bs, Ad-GFP, Adsi-B4 or Ad-RFP). The cells were fixed with 4% paraformaldehyde for 10min, followed by staining with 0.5% periodic acid solution for 5 min at RT. After being rinsed with tap water for 3 min, cells and sections were incubated in the Schiff's reagent for 15 min at RT, followed by

Table 2 List of TqPCR Primers.

Gene	Forward primer	Reverse primer	Accession No.
mouse Gapdh	ACCCAGAAGACTGTGGATGG	CACATTGGGGGTAGGAACAC	NM_008084
mouse Bmp2	TTCTTCAAGGTGAGCGAGGT	TAGTTGGCAGCGTAGCCTTT	NM_007553.3
mouse Bmp3	TCAGCCCCCTGAGAAGAGT	AGGTTCGACCCACTGCTTT	NM_001310677.2
mouse Bmp4	GCGAGCCATGCTAGTTTGA	AAGTGTCGCCTCGAAGTCC	NM_001316360.1
mouse Bmp5	AGATCTGGGATGGCAGGAC	TGGACTATGGCATGGTTGG	NM_007555.4
mouse Bmp6	GCAATCTGTGGGTGGTGAC	CTTGTCGTAAGGGCCGTCT	NM_007556.3
mouse Bmp7	AGGAGCCAACAGACCAACC	TCACGTGCCAGAAGGAAAG	NM_007557.3
mouse Bmp8	CAGAGGCAGGAAACCCTTC	ACCCCATGAAGGACAGAGG	NM_001256019.1
mouse Bmp9	TGAGTCCCATCTCCATCCTC	ACCCACCAGACACAAGAAGG	NM_019506.4
mouse Bmp10	GGTCGTCATGGCTGAACTG	CTCCTCCTCGCTACCGTCT	NM_009756.3
mouse Bmp11	TCGCAGATCCTGAGCAAAC	TTGGAAGTCGTGCAGATCC	NM_010272.2
mouse Bmp12	CCTACCAACCACGCCATC	GGCGGCATCGATGTAGAG	NM_001312876.1
mouse Bmp13	TGGGGGAGGAGGGAATAA	ACGCCAGCTGAGACTTGG	NM_013526.1
mouse Bmp14	GATCCGGTGGCTCTGAAA	GGGGCAGATCCTGCTTTT	NM_008109.3
mouse Bmp15	CTGGCAAGGAGATGAAGCA	CATTTTCGCTCCAATCGTG	NM_009757.5
human BMP2	GGGCATCCTCTCCACAAA	GTCATTCCACCCCACGTC	NM_001200.4
human BMP3	GCTCTACTGGGGTCTTGCTG	ATGAGGCCCCTTTCTCTGTT	NM_001201.4
human BMP4	GCGCCACTCGCTCTATGT	AGGTGGTCAGCCAGTGGA	NM_001202.6
human BMP5	GGAGCTGCTGGGTTCTAGTG	AATGGTCTGGGTCTGTGAGG	NM_001329754.2
human BMP6	TGCAGGAAGCATGAGCTG	GTGCGTTGAGTGGGAAGG	NM_001718.6
human BMP7	GGCAGGACTGGATCATCG	AAGTGGACCAGCGTCTGC	NM_001719.3
human BMP8	TTATCTGCGCCTCCATTTTC	TATGTGCCAACTCTGCTTCG	NM_001720.5
human BMP9	CCTGGGCACAACAAGGAC	CCTTCCCTGGCAGTTGAG	NM_016204.4
human BMP10	AAGAGGACCCCGCTCTACAT	CTGGGAATTCTTGAGGTGGA	NM_014482.3
human BMP11	TTCATGGAGCTTCGAGTCCT	GTTGGCCTTGTAGCGCTTAG	NM_005811.5
human BMP12	TTCATGATGTCGCTTTACCG	ACACGTCGAACAGGAAGCTC	NM_182828.4
human BMP13	GCAGTGAGGAAGGAGACAGG	GCCTACTCATGGGCAATGTT	NM_001001557.4
human BMP14	CCAGGACGATAAGACCGTGT	AGCCCATGTCCTTGAAGTTG	NM_000557.5
human BMP15	GTGAAGCCCTTGACCAGTGT	CACATGGCAGGAGAGATTGA	NM_005448.2
mouse Aldoa	TGACCCCGGAGCAGAAGA	CACACGGTCGTCTGCAGT	NM_001177307.1
mouse Eno3	GTCTGCAAGGCTGGAGCA	TGCGCATGGCTTCCTTGA	NM_001136062.2
mouse Gpi1	TGAAGGAAACCGCCCGAC	TCTTGGCCAGCTGCTTCC	NM_008155.4
mouse Pfkm	GCCCACCTGGAGCACATT	CCTGGTTGCAGGCATGGA	NM_001163487.1
mouse Pgk1	AGGCTGTGGGTCGAGCTA	GGCAGTGTCTCCACCACC	NM_008828.3
mouse Pkm	TGCAACCGAGCTGGGAAG	TCAGGTGCTGCATGCGAA	NM_001253883.1
mouse Pgm2	TGCTGGACCGCTCCTTTG	AGCCGCAAGCCCTGATTT	NM_028132.3
mouse Hk2	CCTGCTCCATCGGTAGCG	TCCTTCCGGAACCGCCTA	NM_013820.3
mouse Ldha	ATGGGAGAGAGGCTGGGG	GCGTCAGTGCCCAGTTCT	NM_001136069.2
mouse Ldhb	GCACGGGAGCTTGTTCCT	ACTCTCCCCCTCCTGCTG	NM_001302765.1
mouse Gsk-3α	GGAACGCCAACCAGGGAA	TGCAATGGCCTCAGGTGG	NM_001031667.1
mouse Gsk-3β	CCCGGCTAACACCACTGG	TCCGAGCATGTGGAGGGA	NM_001347232.1
mouse Nr1h3	AGAGCCTACAGCCCTGCT	ACTGCACAGCTCGTTCCC	NM_001177730.1
mouse Prr5	GATTCCTACGCCGCTCCC	TTCATGCTCGGCCACAGG	NM_001346662.1
mouse Prr5l	GAAGCTGGGTGACGTGCT	CTCACTTGGGCCTGTGGG	NM_001083810.2
mouse Rictor	AGGCACAGTCGCAAGCAT	ATGTGCTGGTGGAGGTGC	NM_030168.3
mouse Mtor	TCATGCCTTTCCTGCGCA	CGGGTTTGGGTCAGGGTC	NM_020009.2
mouse Akt1	AACGGACTTCGGGCTGTG	CACGGCCGTAGTCGTTGT	NM_001165894.1
mouse Akt2	GAGAGGCCACGACCCAAC	CTGGGGGAGCCACACTTG	NM_001110208.2
mouse Akt3	GGACTGGTGGGGCTTAGG	CCCTCCACCAAGGCGTTT	NM_011785.3
mouse Foxo1	CCCTGGACATGCACAGCA	AGCCATTGCAGCTGCTCA	NM_019739.3
mouse Foxo3	TGAAGGCACGGGCAAGAG	TTCTTCTTGGCTGCCCGG	NM_019740.2
mouse Sgk1	CGGTGGACTGGTGGTGTC	GAGGTGCCTTGCCGAGTT	NM_001161845.2

Table 3 List of siRNA Oligos.

Gene	siRNA sequence	Accession No.
mouse Bmp4 siRNA-1	GGTCCAGGAAGAAGAATAA	NR_130973.1
mouse Bmp4 siRNA-2	ACGAAGAACATCTGGAGAA	
mouse Bmp4 siRNA-3	GAGCCATGCTAGTTTGATA	

thorough rinses with tap water. Each assay condition was done in triplicate. The PAS staining results were recorded under a bright field microscope.

Western blotting analysis

Western blotting assay was carried out as previously described.[17,33,43] Briefly, subconfluent MPH cells were infected with Ad-B4, Ad-siB4 and Ad-RFP for 72h. Cell lysates were prepared and subjected to SDS-PAGE and electro-transferred to PVDF membranes, which were blocked and incubated overnight with the primary antibodies against β-ACTIN (1:5000—1:20000 dilution; Proteintech; Cat# 60008-1-Ig), BMP4 (1:1000—1:3000 dilution; Gen Tex; Cat# GTX100874), AKT (1:1000—1:3000 dilution; Gene Tex; Cat# GTX121937), phospho-AKT Ser473 (1:1000—1:3000 dilution; Gene Tex; Cat# GTX128414), GSK-3 β(1:500—1:1000 dilution; Bioss; Cat# bs-0028R), phospho-GSK-3 β Ser9 (1:500—1:1000 dilution; Bioss; Cat# bs-2066R), SGK (1:100 dilution; Santa Cruz Biotechnology; Cat# cs-28338), FOXO1 (1:500—1:1000 dilution; Bioss; Cat# bs-2537R) and phospho-FOXO1 Ser319 (1:500—1:1000 dilution; Bioss; Cat# bs-20095R). After being washed, the membranes were incubated with respective secondary antibodies (1:5000 dilution; ZSGB-BIG; Peroxidase-Conjugated Rabbit anti-Goat IgGor Peroxidase-Conjugated Goat anti-Mouse IgG, Cat#ZB-2306 or 2305) conjugated with horseradish peroxidase. Immune-reactive signals were visualized with the Enhanced Chemiluminescence (ECL) kit (Millipore, USA) using the Bio-Rad ChemiDoc Imager (Hercules, CA).

Ad-B4-mediated BMP4 overexpression *in vivo*

The use and care of experimental animals was approved by the Research Ethics and Regulations Committee of Chongqing Medical University, Chongqing, China. All experimental procedures followed the approved guidelines. The mouse model was established as previously described.[17] Briefly, a total of 40 male 4-week old C57BL/6J were obtained from and housed in the Chongqing Medical University Experimental Animal Research Center. The mice were divided into two groups (20 each), the BMP4 overexpression group was treated with the Ad-B4, and the control group was treated with Ad-GFP.

For the NAFLD model of BMP4 overexpression in liver, a total of 40 male 4-week old C57BL/6J mice were divided into two groups (20 each) and both fed with high-fat diet (HFD). The high-fat diet (HFD) group was fed with the 45% fat diet (Medicience, Yangzhou, China), whereas the control group was fed with 10% fat diet (Table 1). The BMP4 group was treated with the Ad-B4, and the control group was treated with Ad-GFP. Both Ad-B4 and Ad-GFP were intrahepatically injected into the liver area directly as described.[17,35—38] The total amount of virus particles was at 1×10^{10} pfu/injection for each mouse, and the total volume of injection was $<30\mu l$/injection, and the injection was repeated once every 5 days. Ten mice from each group were sacrificed at week 4 and 12, respectively. The retrieved liver tissue was either fixed with 4% paraformaldehyde or snap-frozen in liquid nitrogen for total RNA/protein isolation.

Determination of glucose levels

For cells and tissue samples, 5×10^5 cells were collected and lysed by ultrasonication, or 100 mg liver tissue was grinded, bathed in 95 °C degree water for 10 min. The supernatant was collected for glucose assay using a commercial kit (BC2505, Solarbio, China).

For serum samples, mouse heart blood collection was carried out as previously described.[17] Briefly, animals were first anesthetized by intraperitoneal injection of 3% sodium pentobarbital at 50 mg/kg, an incision was made in upper-middle abdomen across the abdominal and chest cavities to expose the liver and heart, and phlebotomized slowly from the left ventricle until reaching 500 μl for each mouse. The mice were then euthanized. The collected blood was centrifuged at $1000\times g$ for 10 min at RT. The upper portion of the serum samples was collected for assessing serum glucose levels using a commercial kit (F006-1-1, Nanjing Jiancheng Bioengineering Institute, China).

Statistical analysis

All quantitative assays were performed in triplicate and/or repeated three batches of independent experiments. Statistical significances were determined by one-way analysis of variance and the student's t test. $P < 0.05$ was considered statistically significant.

Results

A comprehensive analysis of the 14 types of BMPs indicates that many BMPs are highly expressed in mouse hepatocytes and/or different stages of liver development in mice

As members of TGFβ superfamily, BMPs have pleiotropic effects in development and adult tissue homeostasis.[8,9,44,45] However, their roles in the liver, especially in hepatic glucose metabolism remain to be fully understood. In this study, we first examined the expression profile of 14 types of *Bmps* in the liver at different development stages

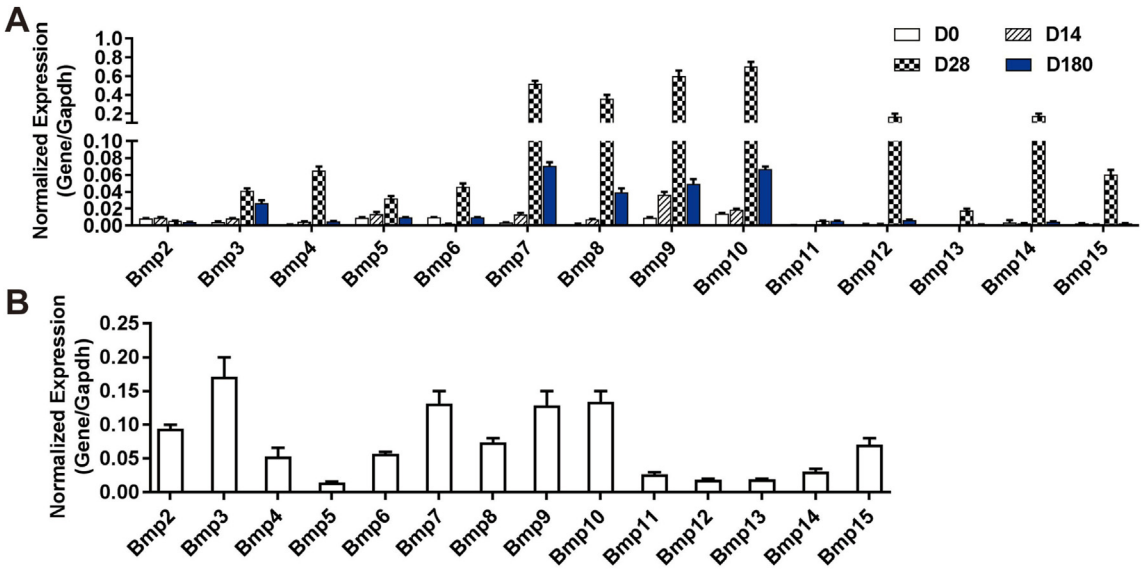

Figure 1 The expression profile of the 14 types of BMPs in mouse liver tissue and hepatocytes. Total RNA was isolated from C57BL/6 male mouse liver tissue at day 0 (D0), day 14 (D14), day 28 (D28) and day 180 (D180) after birth. TqPCR analysis was carried out to assess the expression of the 14 types of *Bmps*. All samples were normalized with *Gapdh* **(A)**. Total RNA was isolated from the MPH cells, and TqPCR analysis was carried out to detect the expression of 14 Bmps **(B)**. All samples were normalized with *Gapdh*. Each assay condition was done in triplicate.

and isolated total RNA from newborn (D0), 14-day-old (D14), 28-day-old (D28) and 180-day-old (D180) mouse liver tissue. Using TqPCR analysis we found that among the 14 types of *Bmps*, *Bmp7*, *8, 9,10,12* and *14* were highly expressed in mouse liver and tended to increase at later stages of liver maturation, whereas *Bmp2*, *3*, *4*, *5*, *6*, 13 and 15 were expressed at low but detectable levels. The expression of all *Bmps* increased gradually from newborn (D0), peaked at 28-day-old (D28) a, and then decreased gradually (Fig. 1A). Furthermore, we analyzed the expression of 14 Bmps in MPH cells *in vitro*, and TqPCR analysis indicated that the expression of *Bmp2*, *3*, *4*, *6*, *7*, *8*, *9*, *10* and *15* were readily detected, while *Bmp5*, *11*, *12*, *13* and *14* were expressed at much lower levels (Fig. 1B). These results indicate multiple members of the BMP family members are highly expressed in mouse hepatocytes and/or at different developmental stages of mouse liver.

BMP4 is one of the most potent BMPs to promote hepatic glycogen accumulation among the 14 types of BMPs, and is able to reduce glucose level in hepatocytes

We previously conducted a comprehensive analysis of the 14 types of BMPs and identified several BMPs (such as BMP2, 4, 6, 7, and 9) as highly adipogenic BMPs in mesenchymal stem cells.[45–47] In order to systematically assess the impact of BMPs on hepatic glucose metabolism, we used the adenoviral vectors expressing the 14 types of human BMPs, designated as Ad-B2 through Ad-B15, to infect MPH cells and verified the adenovirus-mediated BMP expression levels by TqPCR (Fig. S1B), while the adenovirus infection efficiency was verified by examining GFP expression at 48h after infection (Fig. S1A). When the MPH cells were infected with the 14 types of Ad-Bs or Ad-GFP control, we found that BMP4, too much lesser extents BMP2, BMP7 and BMP8, was among the most potent BMPs to induce strong PAS staining (Fig. 2A).

We previously found that BMP4 is up-regulated in oleic acid-induced steatosis in MPH cells and during the development of a mouse model of NAFLD.[17] To fully understand the effect of BMP4 on hepatic glucose metabolism, we constructed an adenoviral vector expressing siRNAs, namely Ad-siB4, which targets the coding region of mouse Bmp4. TqPCR showed that the expression of Bmp4 was effectively silenced by Ad-siB4 in MPH cells (Fig. S1C and D). PAS staining showed that the glycogen accumulation in the MPH cells was effectively blunted by the infection of Ad-siB4 at day 3 (Fig. 2B). Using Ad-B4 or Ad-siB4 to overexpression or silence Bmp4 in MPH cells, then lysated cells, and glucose content test kit results showed that BMP4 reduced the glucose levels in MPH cells from 36 to 48h (Fig. 2C).

We further analyzed the effect of BMP4 on the genes that regulate hepatic glycogen synthesis, such as *Gsk-3*α and *Gsk-3*β, and glucose metabolism, such as *Aldoa* and Nr1h3, and glycolysis and gluconeogenesis, including *Eno3, Gpil, Pfkm, Pgkm, Pkm, Pgm2, Ldha* and *Ldhb*. When the MPH cells were infected with Ad-B4 or Ad-GFP for 36h and 72h, TqPCR analysis revealed that most of glucose metabolism genes were significantly down-regulated at 36h while up-regulated at 72h, compared with that of the GFP control group; Silencing Bmp4 expression in the MPH cells effectively inhibited the expression of the most of glycolysis genes at 36h while increased at 72h, compared with that of the RFP control group (Fig. 2D). Thus, these results suggest that BMP4 may induce the hepatic glycogen

accumulation and reduce glucose levels in hepatocytes through regulating the expression of *Aldoa, Eno3, Gpil, Pfkm, Pgk1, Pgm2, Ldhb, Gsk-3α, Gsk-3β, Nr1h3*.

BMP4 regulates glycogen accumulation and glucose levels through the activation of the mTORC2 signaling pathway in hepatocytes

The mTORC2 signaling pathway plays an important role in governing glycogen synthesis and glucose metabolism, which regulates glucose metabolism genes, including *Pgk1, Pkm, Pgm2, Hk2, Ldha, Gsk-3β and Nr1h3*.[48–50] In order to test whether BMP4 regulates the hepatic glycogen accumulation through mTORC2 signaling pathway, Ad-B4 and Ad-siB4 were used to infect MPH cells for 36h and 72h, TqPCR results showed that BMP4 up-regulated most of essential members of mTORC2 signal pathway, such as *Prr5, Prr51, Rictor, Mtor,* and downstream genes related to glucose metabolism, such as *Akt1, Akt2, Akt3, Foxo1, Foxo3* and *Sgk-1* (Fig. 3A).The hepatic glycogen accumulation induced by BMP4 was blocked by the PI3K(α/β/δ/γ)/mTOR inhibitor PF-04691502 (Selleckchem, Houston, USA) (Fig. 3B) through PAS staining at day 3.

Furthermore, MPH cells were infected with Ad-B4 and treated with PF-04691502 for varied durations, then lysed for glucose assay. The results indicated that glucose levels decreased at 12h and 24h, but increased at 72h (Fig. 3C). We further found that AKT, p-AKT, p-GSK3β were up-regulated, while p-FOXO1 was down-regulated by BMP4 by Western blotting analysis (Fig. 3D), and the densitometry analysis of Western blots was shown in Fig. S2A. Thus, these results suggest that BMP4 may regulate hepatic glycogen and glucose levels through activating or suppressing downstream mediators involved in mTORC2 signaling pathway.

Exogenous BMP4 promotes hepatic glycogen accumulation and decreases glucose levels *in vivo*

To further confirm the effect of BMP4 on hepatic glucose metabolism *in vivo*, we established an exogenous BMP4 overexpression mouse model via intrahepatic adenovirus injection as we previously reported.[17] Experimentally, the 4-week old mice received consecutive intrahepatic injections of high titer Ad-B4 or Ad-GFP once every 5 days for 4 or 12 weeks. Liver tissue and blood samples were collected for further analyses. H & E staining showed that BMP4 overexpression did not cause any obvious histologic changes in mouse liver (Fig. 4A). However, exogenous BMP4 induced the hepatic glycogen accumulation (Fig. 4B), decreased the glucose levels in liver tissue (Fig. 4C) and serum glucose levels (Fig. 4D) both at week 4 and/or 12, interestingly, we observed that BMP4 increased glucose levels in liver tissue at week 12, it can be considered that the body may decompose part of liver glycogen in order to meet energy requirements and maintain the dynamic balance of glucose in the cell. Furthermore, TqPCR results showed that BMP4 effectively regulated the genes expression of glycogen synthesis, such as *Gsk-3α* and *Gsk-3β,* and glucose metabolism, such as *Aldoa and Nr1h3,* glycolysis and gluconeogenesis, *such as Eno3, Gpil, Pfkm, Pgk1, Pkm, Pgm2, Ldha, Ldhb* in liver tissue at weeks 4 and 12 (Fig. 4E).

We further analyzed the effect of exogenous BMP4 on hepatic glucose metabolism during NAFLD development. When the high-fat diet (HFD) 4-week old mice were intrahepatically injected with high titer of Ad-B4 for 4 and 12 weeks as previously described,[17] we found that the expression of glycogen synthesis and glucose metabolism genes changed in the liver tissue after BMP4 treatment (Fig. S2F), although no obviously changes in PAS staining and serum glucose concentrations were observed at week 4 and 12 (Fig. S2D and E).

BMP4 regulates hepatic glucose metabolism through the activation of mTORC2 signaling pathway *in vivo*

Using the liver samples prepared from the mice injected with Ad-B4, we found that the expression of many essential members of mTORC2 signaling pathway, such as *Prr5, Prr51, Rictor, Mtor,* and downstream genes relate to glucose metabolism, such as *Akt1, Akt2, Akt3, Foxo1, Foxo3* and *Sgk-1*were significantly changed after 4 weeks and 12 weeks(Fig. 5A). Western blotting analysis revealed that the BMP4 increased the expression of p-AKT, p-GSK-3β and decreased the expression of p-FOXO1 at week 4 and 12 (Fig. 5B), and the densitometry analysis of Western blots was shown in Fig. S2B and C. Furthermore, IHC staining shown that, p-AKT, p-GSK-3β significantly were high-expression and p-FOXO1 were low-expression regulated by BMP4 (Fig. 5C), compared with the IgG negative controls as shown in Fig. S2G. These results indicated that the activation of mTORC2 signaling by BMP4 in liver tissue.

Discussion

NAFLD is the most prevalent liver disease around the world, with prevalence estimates indicating it affects almost two billion people globally, and fast becoming one of the most common causes of chronic liver disease worldwide, and is now a major cause of liver-related morbidity and mortality.[1,2,4] NAFLD is an example of ectopic fat accumulation, which is usually concomitant with increased gluconeogenesis, decreased glycogen synthesis.[51]

As a member of TGF-β superfamily, bone morphogenetic proteins (BMPs) are precursor proteins with N-terminal signal peptide and C-terminal mature peptide. At present, there are 14 kinds of BMP. In the canonical BMP signaling pathway, BMP binds to cell membrane receptor (BMPR), and activated receptor phosphorylates Smad in cells. After forming a complex with Smad4, it enters the nucleus and binds to the DNA sequence to regulate the transcription of target gene.[52,53] In recent years, studies have shown that some BMPs play an important role in the homeostasis of glucose and lipid metabolism, especially BMP4[7]. Related studies shown that BMP4 can significantly reduce the weight and volume of white fat cells and make white adipocytes undergo "brown adipocyte" characteristic change through PGC1α and promote M2 macrophages to induce beige adipogenesis through p38/MAPK/STAT6/PI3K-Akt signaling pathway,[13,14,54] thus improve insulin

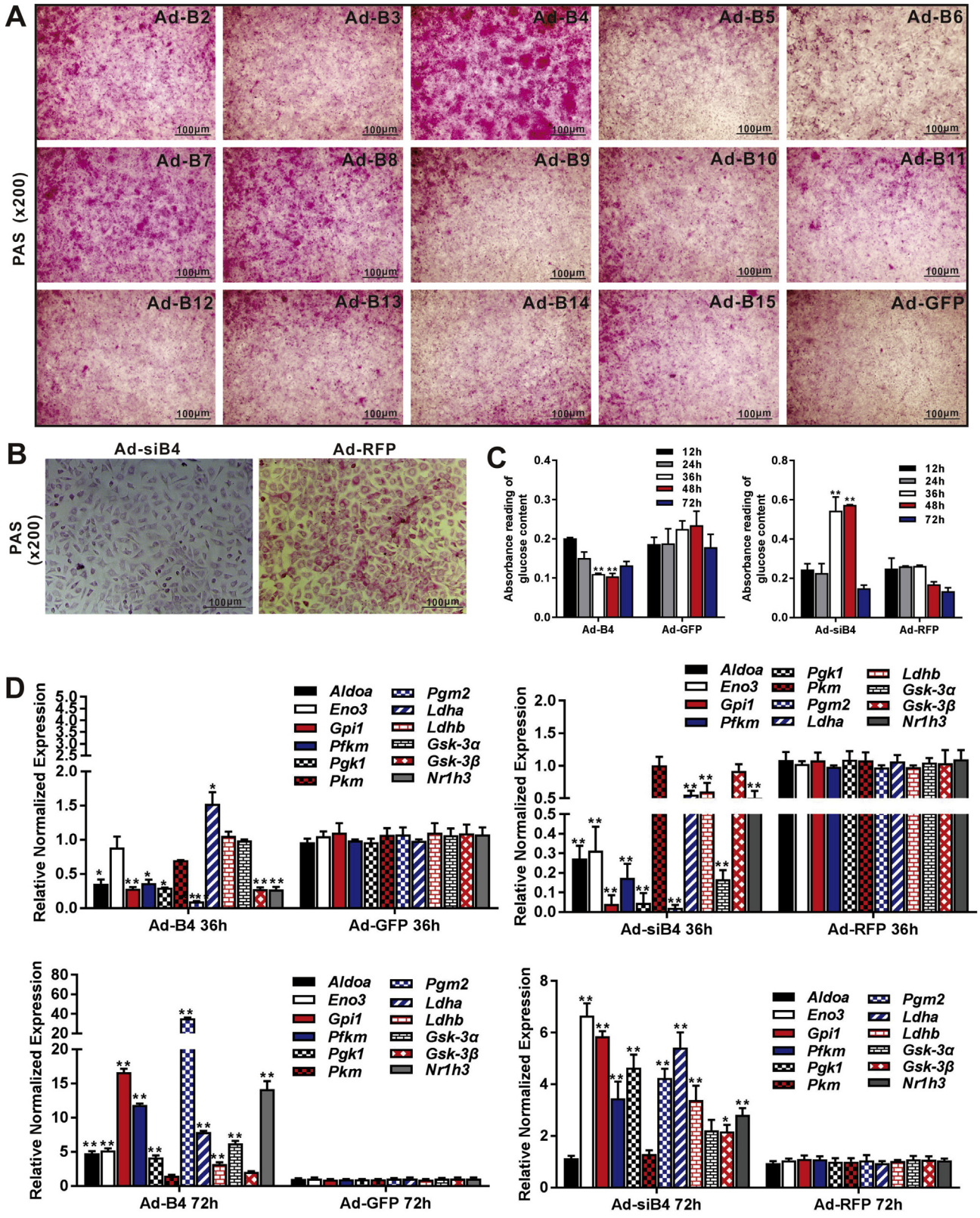

Figure 2 Comprehensive analysis of the 14 types of BMPs in regulating glucose metabolism in hepatocytes. The MPH cells were infected with 14 Ad-Bs and Ad-GFP respectively for 3 days. PAS staining was used to assess hepatic glycogen accumulation (magnification, x200) **(A)** Ad-siB4 and Ad-RFP infected the MPH cells for 3 days, PAS staining was used to assess the hepatic glycogen accumulation (magnification, x200) **(B)** Ad-B4, Ad-GFP, Ad-siB4 and Ad-RFP infected the MPH cells for 12h, 24h, 36h, 48h and 72h, total glucose content in hepatocytes were measured by absorbance reading at 5 time points. "**" $P < 0.01$ Ad-B4 group *vs*. Ad-GFP group, Ad-siB4 group *vs*. Ad-RFP group **(C)** Ad-B4, Ad-GFP, Ad-siB4 and Ad-RFP infected the MPH cells for 36h and 72h, respectively,

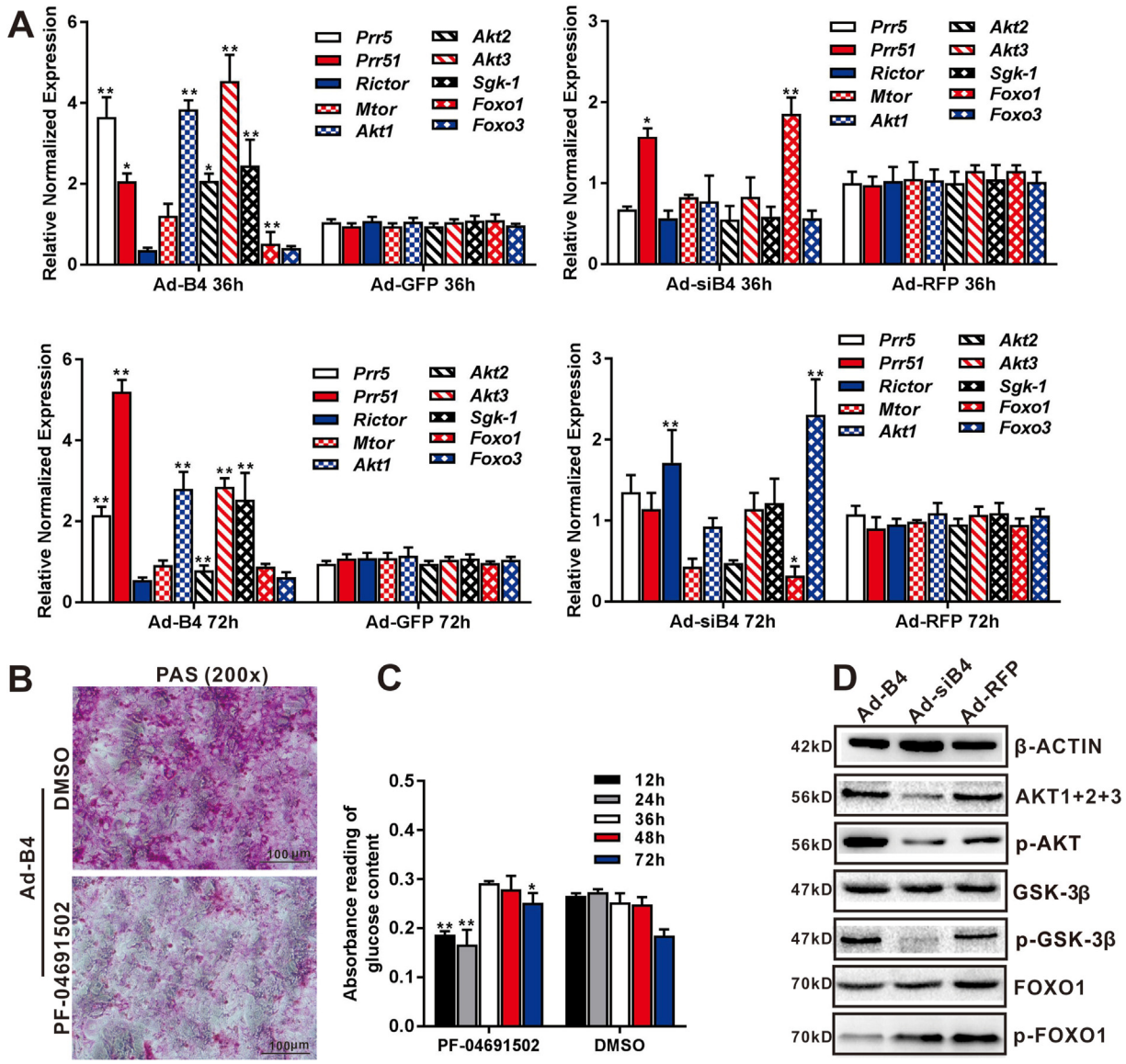

Figure 3 BMP4 regulates hepatic glucose metabolism through mTORC2 signaling. Subconfluent MPH cells were infected with Ad-B4, Ad-GFP, Ad-siB4 and Ad-RFP for 36h and 72h. Total RNA was isolated and TqPCR analysis was carried out to detect the expression of essential members and downstream glucose metabolism related genes of mTORC2 signaling pathway at 36h and 72h, respectively. Relative expression was calculated by dividing the relative expression values (i.e., *gene*/*Gapdh*) in "**" $P < 0.01$, "*" $P < 0.05$, Ad-B4 group *vs*. Ad-GFP group, Ad-siB4 group *vs*. Ad-RFP group **(A)** Subconfluent MPH cells were infected with Ad-B4, treated with the 0.1 mM PI3K($\alpha/\beta/\delta/\gamma$)/mTOR inhibitor PF-04691502 or DMSO vehicle control for 3 days, then subjected to PAS staining (magnification, x200) **(B)** Ad-B4 infected the MPH cells, and treated with PF-04691502 or DMSO for 12h, 24h, 36h, 48h and 72h. Total glucose levels in cells was assessed by absorbance reading at different time points. "**" $P < 0.01$ PF-04691502 group vs. DMSO group **(C)** Subconfluent MPH cells were infected with Ad-B4, Ad-siB4 or Ad-RFP. Total cellular proteins were prepared and subjected to Western blotting to detect the expression or phosphorylation levels of genes related to glucose metabolism regulated by mTORC2 signaling pathway, including AKT1+2+3, p-AKT, GSK-3β, p-GSK-3β, FOXO1, p-FOXO1, while β-ACTIN was used as a loading control **(D)** Each assay condition was done in triplicate. Representative images are shown.

total RNA was isolated and TqPCR analysis was carried out to detect the expression of the genes that govern glycogen synthesis, glucose metabolism, glycolysis and gluconeogenesis respectively. Relative expression was calculated by dividing the relative expression values (i.e., *gene*/*Gapdh*) in "**" $P < 0.01$, "*" $P < 0.05$, Ad-B4 group *vs*. Ad-GFP group, Ad-siB4 group *vs*. Ad-RFP group **(D)**. Each assay condition was done in triplicate. Representative images are shown.

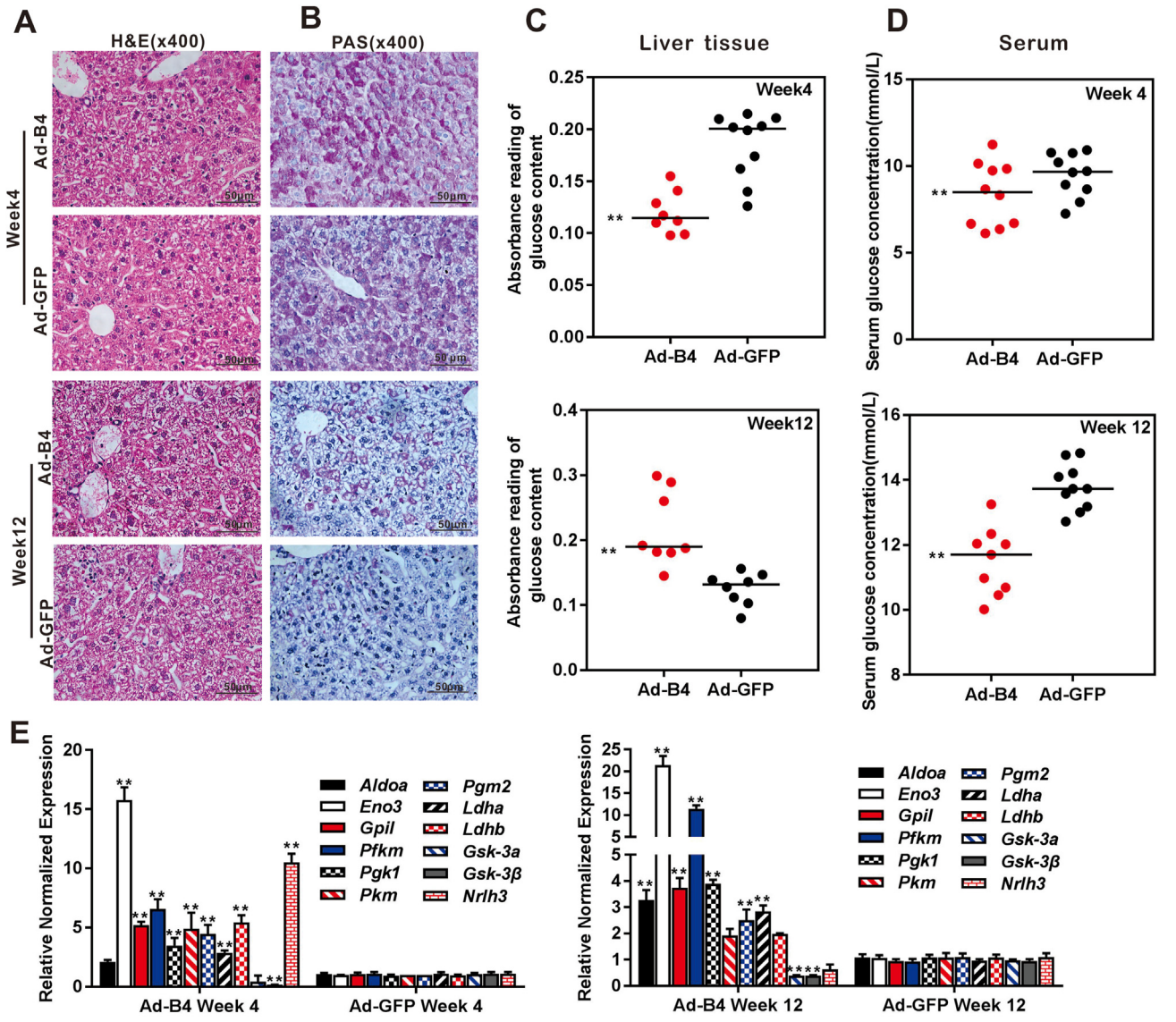

Figure 4 The effect of BMP4 on hepatic glucose concentrations *in vivo*. Recombinant adenovirus Ad-B4 or Ad-GFP was injected intra hepatically into 4-week old C57BL/6 mice (male, $n = 10$/time point/group). The mice were sacrificed after 4 weeks and 12 weeks, respectively. The liver sections were subjected to H & E staining **(A)** and PAS staining **(B)**, both were recorded by light microscopic examination (x400). The liver tissue glucose content **(C)** and serum glucose levels **(D)** were tested with a glucose assay kit, and total RNA was isolated from the liver samples of Ad-B4 group and Ad-GFP group, and TqPCR analysis was carried out to detect the expression of the genes that govern glycogen synthesis, glucose metabolism, glycolysis and gluconeogenesis. Relative expression was calculated by dividing the relative expression values (i.e., *gene*/*Gapdh*) in "**" $P < 0.01$, Ad-B4 group *vs*. Ad-GFP group **(E)**. Each assay condition was done in triplicate. Representative images are shown.

sensitivity, play a protective effect on diet induced obesity and diabetes, and also increase the whole body energy consumption of mice fed with high-fat diet, reduce liver fat and fatty tissue inflammation.[15,16,55] We previously demonstrated that BMP4 expression was elevated during the development of mouse model of NAFLD, and can inhibit hepatic triglyceride/lipid accumulation by suppressing the mTORC1 signaling pathway.[56]

The mechanistic target of rapamycin (mTOR), a kinase that is activated by anabolic signals, plays fundamental roles in regulating metabolism.[48–50] The mTOR forms two distinct complexes, mTOR complex 1 (mTORC1) and mTOR complex 2 (mTORC2), whose activities and substrate specificities are regulated by complex co-factors.[48] Both mTORC1 and mTORC2 harbor several common components: the mTOR kinase, which act as the central catalytic component, mTOR regulatory subunit DEPTOR, the scaffolding protein mLST8, and the Tti1/Tel2 complex, play an important role for mTOR complex assembly and stability. Additionally, each complex contains different subunits that contribute to substrate specificity. The mTORC1 is a complex composed of mTOR, deptor, raptor (a scaffolding protein important for mTORC1 assembly, stability, substrate specificity), pras40 (a factor that blocks mTORC1 activity until growth factor receptor signaling relieves PRAS40-mediated mTORC1

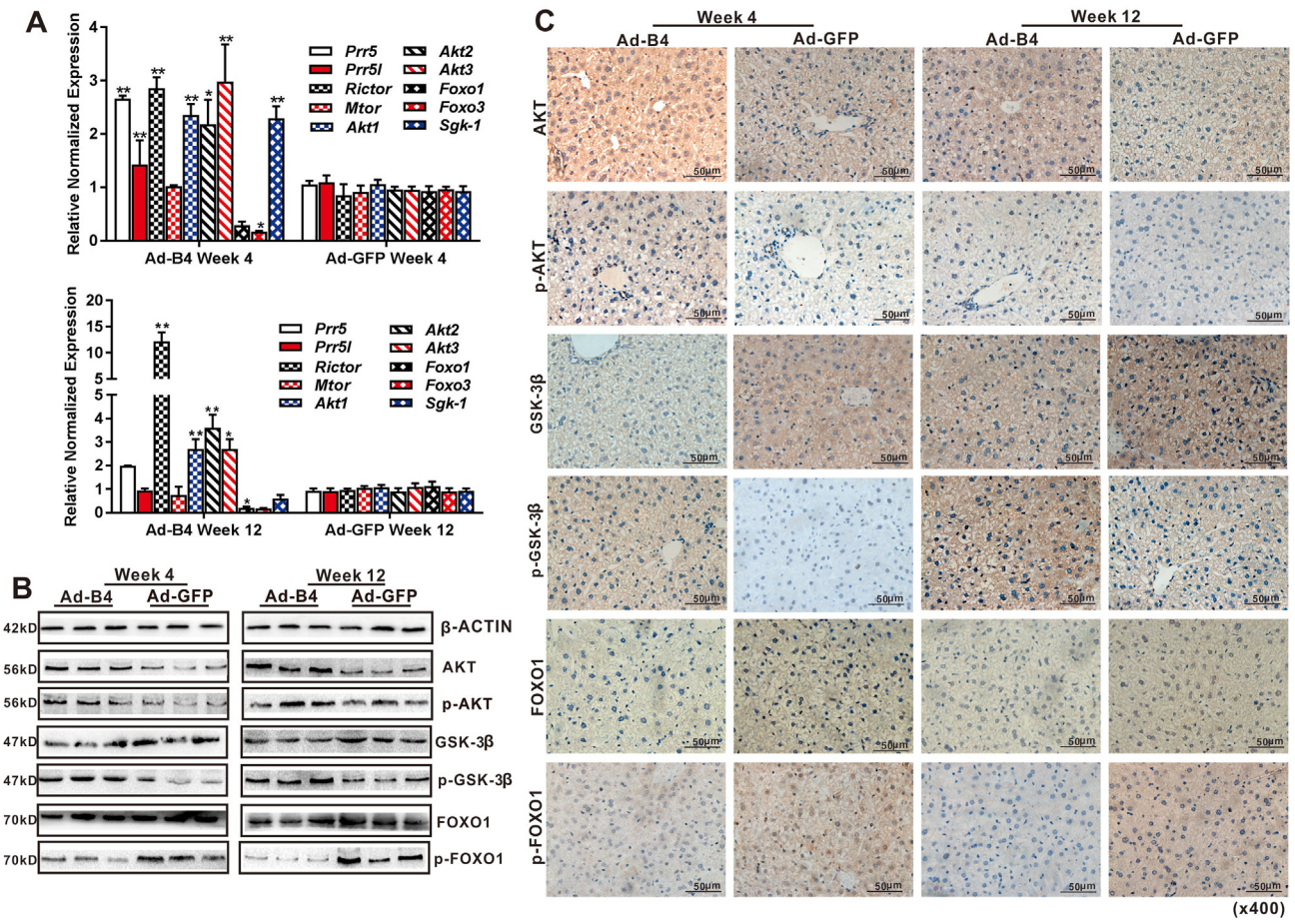

Figure 5 The signaling mechanism of BMP4-regulated glucose metabolism in hepatocytes *in vivo*. Recombinant adenovirus Ad-B4 or Ad-GFP was injected intrahepatically into 4-week old C57BL/6 mice (male, $n = 10$/time point/group). The mice were sacrificed after 4 weeks and 12 weeks, respectively. Total RNA was isolated from the liver of Ad-B4 group and Ad-GFP group. TqPCR analysis was carried out to detect the expression of the members of mTORC2 signaling pathway. Relative expression was calculated by dividing the relative expression values (i.e., *gene*/*Gapdh*) in "**" $P < 0.01$, "*" $P < 0.05$, Ad-B4 group *vs*. Ad-GFP group **(A)** Total tissue proteins were isolated from the liver samples of Ad-B4 group and Ad-GFP group after 4 weeks and 12 weeks, and Western blotting was carried out to detect the expression or phosphorylation level of proteins related to glucose levels regulated by mTORC2 signaling pathway, including AKT1+2+3, p-AKT, GSK-3β, p-GSK-3β, FOXO1, p-FOXO1, and β-ACTIN was used as a loading control **(B)** The liver sections were subjected to IHC staining to detect the expression or phosphorylation level of genes related to glucose metabolism regulated by mTORC2 signaling pathway, including AKT1+2+3, p-AKT, GSK-3β, p-GSK-3β, FOXO1, and p-FOXO1. Staining results were recorded by light microscopic examination (x400) **(C)** Each assay condition was done in triplicate. Representative images are shown.

inhibition) and mlst8, the kinase domains coming in close proximity to one another in the center of the structure and Raptor and mLST8 binding on the periphery. The structure of mTORC2 looks similar to that of mTORC1, although Rictor (a factor which is required for mTORC2 assembly, stability, substrate identification, and subcellular located to the appropriate sites of action) and mSin1 (a key negative regulator of mTORC2 kinase activity) are subunits specific to mTORC2. The differing components and structures of mTORC1 and mTORC2 allow for independent regulation through subcellular localization.[48,57,58] The mTORC1 promotes fat synthesis and storage, inhibits fat consumption and decomposition through activating SREBP to regulate the expression of *FASN*, *ACLY*, *ACC1*, *SCDP1*, *HMGCR*, *LSS*, *SREBP1/2*, etc., and also activating PPAR γ to regulate FABP4, LPL, perilipins, S6K1, CD36 and C/EBPα.[48,57,59,60] According to the classification of KEGG, there are six regulatory pathways in the upstream of mTORC1, which are amino acid pathway, Wnt pathway, TNF-α pathway, insulin signaling pathway (INS/IGF), energy deficit pathway and hypoxia pathway; among them, energy deficiency pathway and hypoxia pathway inhibit mTORC1 activity, and the others activate mTORC1[49,57]. In the regulation pathway of energy deficiency, the production of AMP is increased indirectly due to energy deficiency (low glucose). AMP activates AMPK, and AMPK phosphorylation directly inhibits mTORC1, after phosphorylation, AMPK can also activate the inhibitors of mTORC1, TSC1/2 and tbc1d7, thus indirectly inhibiting the activity of mTORC1[50]. In this process, the decrease of glucose as an initial factor is in a very important position.

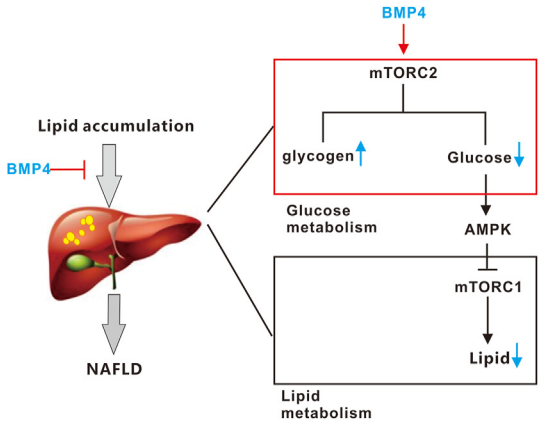

Figure 6 A working model of action for BMP4 in regulating hepatic glucose metabolism.

Unlike mTORC1, the upstream regulation of mTORC2 is not well defined. mTORC2 located at the cell membrane through the mSin1 and mainly phosphorylates AGC kinase family members, including AKT, SGK1, and PKC, to regulate cell growth and metabolism.[61,62] One of the most important role of mTORC2 is the phosphorylation and activation of AKT, a key effector of insulin/PI3K signaling, once active, can phosphorylate and inhibit of several key substrates including the FOXO1/3a transcription factors, the metabolic regulator GSK3β to control whole-body metabolic homeostasis.[50,61–63]

A working mode was shown in Fig. 6, in our previous studies, we demonstrated that BMP4 significantly inhibits hepatic steatosis and lowers serum triglycerides through suppressing mTORC1 signal pathway, playing a protective role against the progression of non-alcoholic fatty liver disease (NAFLD). In this study, we surprisingly identified BMP4 as one of the most potent BMPs among 14 types of BMPs on inducing hepatic glycogen accumulation and reduced the hepatic glucose levels through the activation of mTORC2 signaling pathway. These results indicated there may be a crosstalk between glucose and lipid metabolism regulated by BMP4 through regulate the mTORC1/mTORC2 signal pathway, and the mechanism of the decrease of glucose is the initial factor to inhibit the mTORC1 signal pathway through activating AMPK by BMP4 need further to been verified.

Collectively, our findings strongly suggest that BMP4 may play a very important role in regulating hepatic glucose metabolism. This knowledge should help us to understand the molecular pathogenesis of NAFLD, and as one of the 14 kinds of BMPs, BMP4 plays a key role in the glycose and lipid metabolism of hepatocytes, and which can be used as a potential clinical diagnostic marker and drug treatment target for NAFLD.

Conflict of Interests

The authors declare they have no competing interesting.

Funding

The reported study was supported in part by research grants from the 2017 Chongqing Postdoctoral Innovation Talent Support Program (Chongqing Human Resources and Social Security Bureau No. 356) (JMF), the 64th China Postdoctoral Science Fund (No. 2018M643426) (JMF), the 2019 Chongqing Support Program for Entrepreneurship and Innovation (Chongqing Human Resources and Social Security Bureau No. 288) (JMF), the 2019 Science and Technology Research Plan Project of Chongqing Education Commission (KJQN201900410) (JMF), the 2019 Youth Innovative Talent Training Program of Chongqing Education Commission (CY200409) (JMF), the 2019 Funding for Postdoctoral Research (Chongqing Human Resources and Social Security Bureau No. 298) (JMF), and the National Key Research and Development Program of China (2016YFC1000803 and 2011CB707906). Funding sources were not involved in the study design; in the collection, analysis and interpretation of data; in the writing of the report; and in the decision to submit the paper for publication.

Appendix A. Supplementary data

Supplementary data to this article can be found online at https://doi.org/10.1016/j.gendis.2020.11.004.

Abbreviations

Ad-B4	Adenoviral vector expressing human BMP4
Ad-GFP	Adenoviral vector expressing the green fluorescent protein (GFP)
Ad-RFP	Adenoviral vector expressing the red fluorescent protein (RFP)
Ad-siB4	Adenoviral vector expressing three siRNAs that silence mouse Bmp4
AKT1	AKT serine/threonine kinase 1
AKT2	AKT serine/threonine kinase 2
AKT3	AKT serine/threonine kinase 3
Aldoa	aldolase, fructose-bisphosphate A
BMP/Bmp4	bone morphogenetic protein 4
Eno3	enolase 3
Foxo1	forkhead box O1
Foxo3	forkhead box O3
Gpi1	glucose-6-phosphate isomerase 1
Gsk-3α	glycogen synthase kinase 3 alpha
Gsk-3β	glycogen synthase kinase 3 beta
H & E	hematoxylin and eosin
Hk2	hexokinase 2
IHC	immunohistochemistry
Ldha	lactate dehydrogenase A
Ldhb	lactate dehydrogenase B
Mtor	mechanistic target of rapamycin kinase
NAFLD	non-alcoholic fatty liver disease
Nr1h3	nuclear receptor subfamily 1 group H member 3
PAS staining	periodic acid Schiff staining
Pfkm	phosphofructokinase, muscle
Pgk1	phosphoglycerate kinase 1
Pgm2	phosphoglucomutase 2
Pkm	pyruvate kinase M1/2
Prr5	proline rich 5
Prr5l	proline rich 5 like
Rictor	RPTOR independent companion of MTOR, complex 2
Sgk1	serum/glucocorticoid regulated kinase 1
TqPCR	touchdown quantitative real-time PCR

References

1. Younossi ZM, Koenig AB, Abdelatif D, Fazel Y, Henry L, Wymer M. Global epidemiology of nonalcoholic fatty liver disease-Meta-analytic assessment of prevalence, incidence, and outcomes. *Hepatology*. 2016;64(1):73—84.
2. Whalley S, Puvanachandra P, Desai A, Kennedy H. Hepatology outpatient service provision in secondary care: a study of liver disease incidence and resource costs. *Clin Med (Lond)*. 2007; 7(2):119—124.
3. Mittendorfer B, Magkos F, Fabbrini E, Mohammed BS, Klein S. Relationship between body fat mass and free fatty acid kinetics in men and women. *Obesity (Silver Spring)*. 2009;17(10): 1872—1877.
4. Younossi ZM, Marchesini G, Pinto-Cortez H, Petta S. Epidemiology of nonalcoholic fatty liver disease and nonalcoholic steatohepatitis: implications for liver transplantation. *Transplantation*. 2019;103(1):22—27.
5. Byrne CD, Targher G. NAFLD: a multisystem disease. *J Hepatol*. 2015;62(1 Suppl):S47—S64.
6. Mehal WZ. The Gordian Knot of dysbiosis, obesity and NAFLD. *Nat Rev Gastroenterol Hepatol*. 2013;10(11):637—644.
7. Salazar VS, Gamer LW, Rosen V. BMP signalling in skeletal development, disease and repair. *Nat Rev Endocrinol*. 2016; 12(4):203—221.
8. Wang RN, Green J, Wang Z, et al. Bone Morphogenetic Protein (BMP) signaling in development and human diseases. *Genes Dis*. 2014;1(1):87—105.
9. Mostafa S, Pakvasa M, Coalson E, et al. The wonders of BMP9: from mesenchymal stem cell differentiation, angiogenesis, neurogenesis, tumorigenesis, and metabolism to regenerative medicine. *Genes Dis*. 2019;6(3):201—223.
10. Zhang L, Luo Q, Shu Y, et al. Transcriptomic landscape regulated by the 14 types of bone morphogenetic proteins (BMPs) in lineage commitment and differentiation of mesenchymal stem cells (MSCs). *Genes Dis*. 2019;6(3):258—275.
11. Bragdon B, Moseychuk O, Saldanha S, King D, Julian J, Nohe A. Bone morphogenetic proteins: a critical review. *Cell Signal*. 2011;23(4):609—620.
12. Zhang F, Song J, Zhang H, et al. Wnt and BMP signaling crosstalk in regulating dental stem cells: implications in dental tissue engineering. *Genes Dis*. 2016;3(4):263—276.
13. Qian SW, Tang Y, Li X, et al. BMP4-mediated brown fat-like changes in white adipose tissue alter glucose and energy homeostasis. *Proc Natl Acad Sci U S A*. 2013;110(9): E798—E807.
14. Qian SW, Wu MY, Wang YN, et al. BMP4 facilitates beige fat biogenesis via regulating adipose tissue macrophages. *J Mol Cell Biol*. 2019;11(1):14—25.
15. Gustafson B, Hammarstedt A, Hedjazifar S, et al. BMP4 and BMP antagonists regulate human white and beige adipogenesis. *Diabetes*. 2015;64(5):1670—1681.
16. Modica S, Straub LG, Balaz M, et al. Bmp4 promotes a Brown to white-like adipocyte shift. *Cell Rep*. 2016;16(8):2243—2258.
17. Peng Q, Chen B, Wang H, et al. Bone morphogenetic protein 4 (BMP4) alleviates hepatic steatosis by increasing hepatic lipid turnover and inhibiting the mTORC1 signaling axis in hepatocytes. *Aging (Albany NY)*. 2019;11(23):11520—11540.
18. Cui J, Zhang W, Huang E, et al. BMP9-induced osteoblastic differentiation requires functional Notch signaling in mesenchymal stem cells. *Lab Invest*. 2019;99(1):58—71.
19. Wei Q, Fan J, Liao J, et al. Engineering the rapid adenovirus production and amplification (RAPA) cell line to expedite the generation of recombinant adenoviruses. *Cell Physiol Biochem*. 2017;41(6):2383—2398.
20. Seglen PO. Preparation of isolated rat liver cells. *Methods Cell Biol*. 1976;13(13):29—83.
21. Liu W, Deng Z, Zeng Z, et al. Highly expressed BMP9/GDF2 in postnatal mouse liver and lungs may account for its pleiotropic effects on stem cell differentiation, angiogenesis, tumor growth and metabolism. *Genes Dis*. 2020;7(2): 235—244.
22. Fan J, Feng Y, Zhang R, et al. A simplified system for the effective expression and delivery of functional mature microRNAs in mammalian cells. *Cancer Gene Ther*. 2020;27(6):424—437.
23. Fan J, Wei Q, Liao J, et al. Noncanonical Wnt signaling plays an important role in modulating canonical Wnt-regulated stemness, proliferation and terminal differentiation of hepatic progenitors. *Oncotarget*. 2017;8(16):27105—27119.
24. He TC, Zhou S, da Costa LT, Yu J, Kinzler KW, Vogelstein B. A simplified system for generating recombinant adenoviruses. *Proc Natl Acad Sci U S A*. 1998;95(5):2509—2514.
25. Luo J, Deng ZL, Luo X, et al. A protocol for rapid generation of recombinant adenoviruses using the AdEasy system. *Nat Protoc*. 2007;2(5):1236—1247.
26. Cheng H, Jiang W, Phillips FM, et al. Osteogenic activity of the fourteen types of human bone morphogenetic proteins (BMPs). *J Bone Joint Surg Am*. 2003;85(8):1544—1552.
27. Lee CS, Bishop ES, Zhang R, et al. Adenovirus-mediated gene delivery: potential applications for gene and cell-based therapies in the new era of personalized medicine. *Genes Dis*. 2017;4(2):43—63.
28. Luo Q, Kang Q, Song WX, et al. Selection and validation of optimal siRNA target sites for RNAi-mediated gene silencing. *Gene*. 2007;395(1—2):160—169.
29. Deng F, Chen X, Liao Z, et al. A simplified and versatile system for the simultaneous expression of multiple siRNAs in mammalian cells using Gibson DNA Assembly. *PLoS One*. 2014; 9(11), e113064.
30. Shu Y, Wu K, Zeng Z, et al. A simplified system to express circularized inhibitors of miRNA for stable and potent suppression of miRNA functions. *Mol Ther Nucleic Acids*. 2018;13: 556—567.
31. Wang X, Yuan C, Huang B, et al. Developing a versatile shotgun cloning strategy for single-vector-based multiplex expression of short interfering RNAs (siRNAs) in mammalian cells. *ACS Synth Biol*. 2019;8(9):2092—2105.
32. Yu X, Chen L, Wu K, et al. Establishment and functional characterization of the reversibly immortalized mouse glomerular podocytes (imPODs). *Genes Dis*. 2018;5(2):137—149.
33. Wang H, Cao Y, Shu L, et al. Long non-coding RNA (lncRNA) H19 induces hepatic steatosis through activating MLXIPL and mTORC1 networks in hepatocytes. *J Cell Mol Med*. 2020;24(2): 1399—1412.
34. Zhao C, Wu N, Deng F, et al. Adenovirus-mediated gene transfer in mesenchymal stem cells can be significantly enhanced by the cationic polymer polybrene. *PLoS One*. 2014; 9(3), e92908.
35. Kang Q, Sun MH, Cheng H, et al. Characterization of the distinct orthotopic bone-forming activity of 14 BMPs using recombinant adenovirus-mediated gene delivery. *Gene Ther*. 2004;11(17):1312—1320.
36. Mehta V, Kang Q, Luo J, He TC, Haydon RC, Mass DP. Characterization of adenovirus-mediated gene transfer in rabbit flexor tendons. *J Hand Surg Am*. 2005;30(1):136—141.
37. Paul R, Haydon RC, Cheng H, et al. Potential use of Sox9 gene therapy for intervertebral degenerative disc disease. *Spine (Phila Pa 1976)*. 2003;28(8):755—763.
38. Bolt P, Clerk AN, Luu HH, et al. BMP-14 gene therapy increases tendon tensile strength in a rat model of Achilles tendon injury. *J Bone Joint Surg Am*. 2007;89(6):1315—1320.
39. Huang E, Bi Y, Jiang W, et al. Conditionally immortalized mouse embryonic fibroblasts retain proliferative activity without compromising multipotent differentiation potential. *PLoS One*. 2012;7(2), e32428.

40. Bi Y, He Y, Huang J, et al. Functional characteristics of reversibly immortalized hepatic progenitor cells derived from mouse embryonic liver. *Cell Physiol Biochem*. 2014;34(4):1318—1338.
41. Bi Y, Huang J, He Y, et al. Wnt antagonist SFRP3 inhibits the differentiation of mouse hepatic progenitor cells. *J Cell Biochem*. 2009;108(1):295—303.
42. Huang J, Bi Y, Zhu GH, et al. Retinoic acid signalling induces the differentiation of mouse fetal liver-derived hepatic progenitor cells. *Liver Int*. 2009;29(10):1569—1581.
43. Huang B, Huang LF, Zhao L, et al. Microvesicles (MIVs) secreted from adipose-derived stem cells (ADSCs) contain multiple microRNAs and promote the migration and invasion of endothelial cells. *Genes Dis*. 2020;7(2):225—234.
44. Luu HH, Song WX, Luo X, et al. Distinct roles of bone morphogenetic proteins in osteogenic differentiation of mesenchymal stem cells. *J Orthop Res*. 2007;25(5):665—677.
45. Lamplot JD, Qin J, Nan G, et al. BMP9 signaling in stem cell differentiation and osteogenesis. *Am J Stem Cells*. 2013;2(1):1—21.
46. Kang Q, Song WX, Luo Q, et al. A comprehensive analysis of the dual roles of BMPs in regulating adipogenic and osteogenic differentiation of mesenchymal progenitor cells. *Stem Cell Dev*. 2009;18(4):545—559.
47. Tang N, Song WX, Luo J, et al. BMP-9-induced osteogenic differentiation of mesenchymal progenitors requires functional canonical Wnt/beta-catenin signalling. *J Cell Mol Med*. 2009;13(8B):2448—2464.
48. Caron A, Richard D, Laplante M. The roles of mTOR complexes in lipid metabolism. *Annu Rev Nutr*. 2015;35:321—348.
49. Lamming DW, Sabatini DM. A Central role for mTOR in lipid homeostasis. *Cell Metab*. 2013;18(4):465—469.
50. Saxton RA, Sabatini DM. mTOR signaling in growth, metabolism, and disease. *Cell*. 2017;168(6):960—976.
51. Younossi Z, QM A, Marietti M, et al. Global burden of NAFLD and NASH: trends, predictions, risk factors and prevention. *Nat Rev Gastroenterol Hepatol*. 2018;15(1):11—20.
52. Wang W, Rigueur D, Bone KMLJ. TGFβ as a gatekeeper of BMP action in the developing growth plate. 2020;137, e115439.
53. Yang J, Ueharu H, Mishina Y. Energy metabolism: A newly emerging target of BMP signaling in bone homeostasis. *Bone*. 2019;138, e115467.
54. Qian SW, Wu MY, Wang YN, et al. BMP4 facilitates beige fat biogenesis via regulating adipose tissue macrophages. *J Mol Cell Biol*. 2019;11(1):14—25.
55. Hoffmann JM, Grunberg JR, Church C, et al. BMP4 gene therapy in mature mice reduces BAT activation but protects from obesity by browning subcutaneous adipose tissue. *Cell Rep*. 2017;20(5):1038—1049.
56. Peng Q, Chen B, Wang H, Zhu Y, Aging JFJ. Bone morphogenetic protein 4 (BMP4) alleviates hepatic steatosis by increasing hepatic lipid turnover and inhibiting the mTORC1 signaling axis in hepatocytes. *Aging (Albany NY)*. 2019;11(23):11520—11540.
57. Han J, Wang Y. mTORC1 signaling in hepatic lipid metabolism. *Protein Cell*. 2018;9(2):145—151.
58. Inoki K, Kim J, Guan KL. AMPK and mTOR in cellular energy homeostasis and drug targets. *Annu Rev Pharmacol Toxicol*. 2012;52:381—400.
59. Petersen MC, Vatner DF, Shulman GI. Regulation of hepatic glucose metabolism in health and disease. *Nat Rev Endocrinol*. 2017;13(10):572—587.
60. Peterson TR, Sengupta SS, Harris TE, et al. mTOR complex 1 regulates lipin 1 localization to control the SREBP pathway. *Cell*. 2011;146(3):408—420.
61. Guertin DA, Stevens DM, Thoreen CC, et al. Ablation in mice of the mTORC components raptor, rictor, or mLST8 reveals that mTORC2 is required for signaling to Akt-FOXO and PKCalpha, but not S6K1. *Dev Cell*. 2006;11(6):859—871.
62. Hagiwara A, Cornu M, Cybulski N, et al. Hepatic mTORC2 activates glycolysis and lipogenesis through Akt, glucokinase, and SREBP1c. *Cell Metab*. 2012;15(5):725—738.
63. García-Martínez JM, Alessi DR. mTOR complex 2 (mTORC2) controls hydrophobic motif phosphorylation and activation of serum- and glucocorticoid-induced protein kinase 1 (SGK1). *Biochem J*. 2008;416(3):375—385.